




Investigation an environmentally friendly method under magnetic field as a green solvent for the synthesis of brookite phase nanoparticles at room temperature

Yahya Absalan^{1,*} , Mostafa Gholizadeh^{1,*}, Vladimir V. Kopylov², Leonid A. Butusov², Valiollah Bagherzadeh³, Seyed Hamid Hosseini Sajed³, and Olga V. Kovalchukova⁴

¹Department of Chemistry, Faculty of Science, Ferdowsi University of Mashhad, Mashhad, Islamic Republic of Iran

²Institute of Innovative Engineering Technologies, RUDN University, 6, Miklukha-Maklaya st, Moscow, Russian Federation 117198

³Quality Paints and Chemicals Section, Factory of Iran Khodro Khorasan, kilometer 55, Binalood, Islamic Republic of Iran

⁴General Chemistry Department, RUDN University, 6, Miklukha-Maklaya st, Moscow, Russian Federation 117198

Received: 16 January 2021

Accepted: 1 April 2021

© The Author(s), under exclusive licence to Springer Science+Business Media, LLC, part of Springer Nature 2021

ABSTRACT

TiO₂ nanoparticles in the brookite phase were synthesized within an environmentally friendly method by magnetized water obtained by the US-patent magnetizing device (US10507450B2), which changes the properties of all types of the solvents with no limitation (protic or aprotic). Furthermore, this study is the first report on the synthesis of brookite TiO₂ nanoparticle through magnetized water at room temperature. The procedure was tested by five different water; ordinary, 15, 30, 45, and 60 min-magnetized water. The products were analyzed by various techniques including XRD, FESEM, ICP, BJH-plot, t-plot, Langmuir plot, BET, TEM, and FTIR. The result showed that the products obtained from 30 min-magnetized water were the most properly indexed TiO₂ brookite phase with high surface activity.

1 Introduction

TiO₂ nanoparticles are one of the most proper and popular semiconductors whose applications cover diverse industrial areas including photocatalysis [1, 2], thin-film, sunscreen, photovoltaic, electrodes [3, 4], sensors [5, 6], and drug delivery [7, 8]. In this regard, TiO₂ nanoparticles have been prepared

through different methods, including sol-gel [9], inverse micelle [10, 11], hydrothermal [12], straight oxidation [13–15], chemical vapor deposition [16–18], physical vapor deposition [19–21], electrochemical accumulation [22–24], sonochemical [25], microwave [26–28], and organometallic complex compounds [29–34]. However, almost all of the mentioned methods require high temperature (usually more

Address correspondence to E-mail: Yahyaabsalan2014@gmail.com; m_gholizadeh@um.ac.ir

than 500 °C) [35]. Some of them even need organic solvents which may contaminate the environment. In addition, in the large scale consuming high energy neither environmentally nor economically is affordable. Motivated by the mentioned drawbacks, we tried to find an alternative method to avoid high temperatures and organic solvent in order to have a cleaner environment.

Magnetized solvents have been used for more than 50 years in different fields such as chemical reactions [36–44], concrete [45–48], poultry [49, 50], oil [51], medicine [49], and agriculture [52]. In all the mentioned areas magnetized solvents, especially water, consumed lower energy; hence they are cost-effective and more environmentally friendly.

In all cases, however, a magnetized component is used to magnetize the solvent as the device cannot do that. Here, we invented a device to magnetize the solvent; through influencing magnetization, the properties of the solvent can be changed. Moreover, other devices fail to magnetize all the organic and aqueous solvents due to some limitations such as corrosion and combustion, therefore, water is the only solvent for magnetization. Recently, we registered a US-patent magnetizing device [53] (Fig. 1), capable of magnetizing different solvents (with various hydrogen bond angles), with no limitation, through the magnetic field to obtain various properties. The important point is that this device does not magnetize the solvents, but it rather alters their structures and behaviors. By controlling the condition, it is possible to use these new properties in different areas. In our previous work, we reviewed application of magnetized water as green technology, published in journal of cleaner production [54]. Here, in this experiment, TiO₂ brookite phase nanoparticles were synthesized from an utter environmentally friendly method by means of room temperature and magnetized water using the developed device which worked the same as a centrifuge (Fig. 1). However, the purpose was quite different, and it was employed for magnetizing solvent.

2 The operation of the device (Micro device)

The device operates basing on the influence of electromagnet rule introduced by Michael Faraday in 1832. After passing through the device, water is

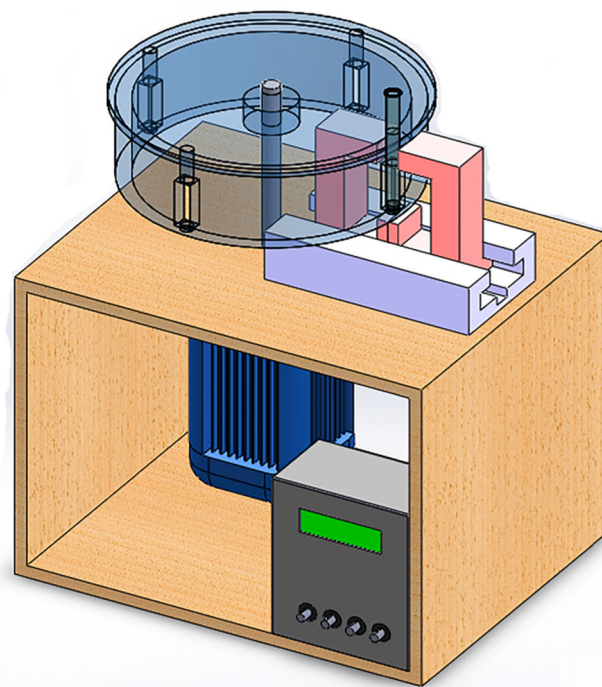


Fig. 1 Micro magnetic device

affected by the magnetic energy, and hence the physical and electric properties of its colloid particles such as sodium carbonate molecules, salts, and other minerals will be altered. It changes the electrical arrangement of the ions and ultimately prevents sedimentation. Also, the magnetic energy can reduce the surface tension by 10%, making an unfavorable condition for the formation of sticky sediments giving rise to magnetized water. In this experiment, a lab-scale microdevice was used for the following purposes:

1. Organic reactions are very expensive due to using organic solvents, thus they will not be affordable if high volumes of solvent are employed for magnetizing.
2. Magnetizing high amounts of solvent but just using 5 or 10 cc is energetically not green.
3. Avoiding solvent waste due to applying device with various volumes (Fig. 2):
 1. Sample tube
 2. Strong magnets
 3. U-shape groove
 4. Magnetic field strength regulator
 5. Electro motor
 6. Bearing
 7. Invertor

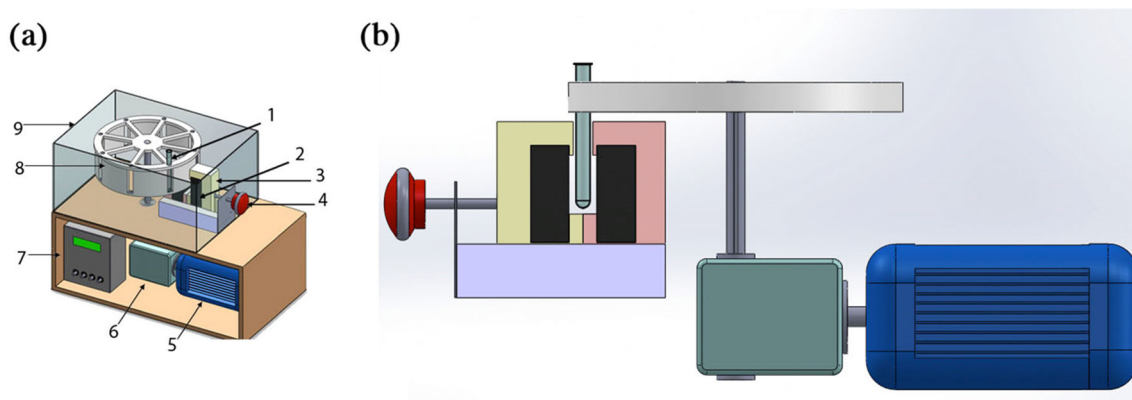


Fig. 2 **a** The general scheme of the micro magnetizing fluids apparatus, **b** interior schematic of the microdevice

8. Rotating table
9. Screen protection

A rotary motor (1500 round per min, frequency (50 Hz), and power (1HP)) was used to construct this device to raise the fluid speed in the magnetic field to the desired level. By enhancing the particle speed in the magnetic field the influenced magnetic property will be increased.

This device has a plate to hold the fluid sample; the material is PTFE = Poly Tetra Fluoro Ethylene which rotates around the axle out of the engine. The device is similar to a centrifuge.

Two jaws made of PTFE were responsible for holding a permanent magnet, which is made of neodymium nickel alloy with a dimension of $100 \times 50 \times 40 \text{ mm}^3$ and power of 15,000 Gauss. These jaws were ambulant to prepare different intensities of the magnetic field between 2000 and 6500 Gauss. The electromagnetic field can be increased by 20,000 Gauss. An electronic part was considered to adjust the engine speed. It is one of the most important parameters because by changing the speed of the engine and power of the magnetic field, it is possible to study new subjects on the chemical reaction.

3 Experiment

3.1 Material

TiCl_3 was purchased from the Aldrich with no further purification (> 98%). NaOH also was purchased with high quality (> 99%) from Aldrich.

3.2 Synthesis of TiO_2

25 ml of deionized water was poured to the glass tube embedded in the device and the round of the engine was set by the inverter (Rotary motor: 1500 round per min, frequency: 30 Hz, and power: 1HP), then the device was turned on and the magnetic process was started. Different samples were studied: ordinary as blank, 15 min magnetized, 30 min magnetized, 45 min magnetized, and 60 min-magnetized water and the following method was tested for all the obtained products).

0.15 mol/l TiCl_3 (15%) dissolved in HCl (10–15%) was added to 25 ml pre-magnetized water under stirring; the experiment was carried under air at a room temperature. The color changed to light blue-violet. Further pH was set between 6 and 7 (NaOH was used), and a precipitate was obtained. Except for the ordinary water, the precipitation took place, however, the color was different from white to cream for 15, 30, 45, and 60 min-magnetized water, respectively. The precipitates were transferred to the oven to be dried at $50 \text{ }^\circ\text{C}$ for 24 h. The sample with the ordinary water was dried. Finally, the precipitates were washed several times with an acidic solution (PH: 1) and then by distilled water to eliminate salts, and finally they were dried under nitrogen atmosphere, and transferred for the corresponding analyses.

3.3 Characterizations

XRD patterns were recorded by GNR Explorer advance using 1.541 Å (Cu-K α). The FT-IR spectra were obtained by Avatar 370 spectrophotometer (in the range of $400\text{--}4000 \text{ cm}^{-1}$). BET analysis was

employed to measure the surface activity of the nanoparticles using capillary condensation of nitrogen at 77 K on a micrometric Belsorp-mini II. To estimate the mesoporosity and pore size distribution, the Barrett-Joyner-Halenda method (BJH) was applied. The microscopic images of the nanoparticles were detected by a FESEM microscope (TESCAN BRNO-Mira3 LMU) to study the morphology of the nanoparticles, was accompanied by EDX analysis. TEM images were taken by LEO 912AB through dispersing the samples into ethanol.

4 Results and discussion

4.1 Results

Figure 3 illustrates the XRD pattern of TiO₂ samples. Accordingly, no specific peak was observed when ordinary water was used. However, peaks appeared, and crystallites formed by water magnetization. The samples magnetized for 15 min (sample 1) and 30 min (sample 2) were the best solvents due to the growth of peaks which indicates crystallinity. In the case of 30 min-magnetized water (Fig. 3c), the XRD pattern exhibited diffraction peaks at $2\theta = 25.68, 32.85, 46.08, 55.29, 65.308, \text{ and } 75.16$ deg. The index pattern of the samples is observable in Fig. 3b and c. According to the index, it is an orthorhombic brookite phase, consistent with the standard XRD data for brookite TiO₂ (JCPDS 76–1934). All diffraction peaks are sharp, illustrating a highly crystalline sample. Waters magnetized for 45 min and 60 min were not suitable as the peaks were reduced or vanished.

Crystalline size of the TiO₂ nanoparticle obtained from the 30 min-magnetized water was calculated by the Scherer Eq. (1) as 12 nm:

$$D = \frac{k\lambda}{\beta \cos\theta} \quad (1)$$

Figure 4 illustrates the FESEM images of the samples. For the ordinary water and those magnetized for 45, and 60 min, no shape was observed. Even it was hard to detect a 3D structure. However, the diamond plate shape of brookite, as dominant structure, and spherical anatase shape related to TiO₂ nanoparticle were observed in the case of the 30 min-magnetized water.

EDX analysis of the TiO₂ nanoparticle was carried out to analyze oxygen and titanium elements

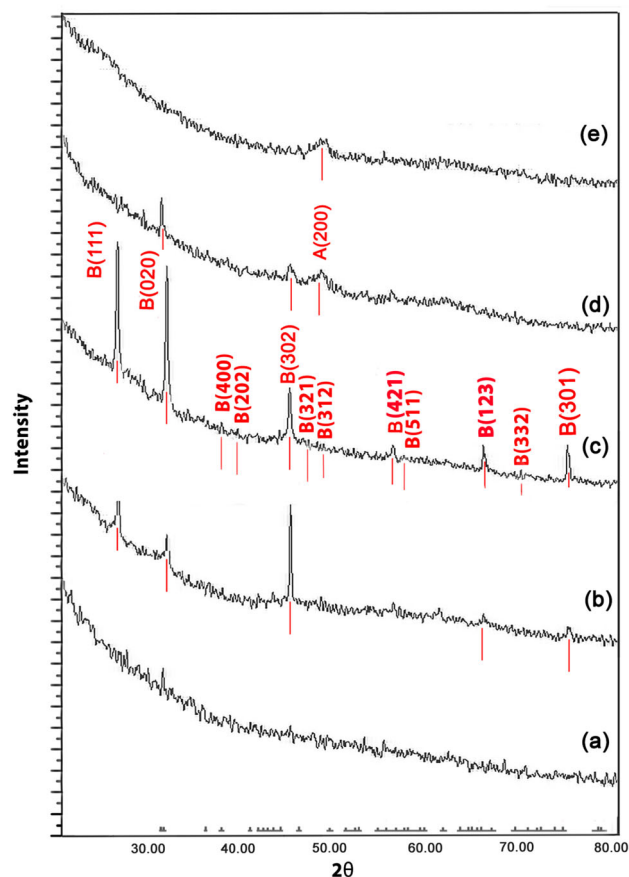


Fig. 3 XRD pattern; **a** ordinary water, **b** magnetized water (15 min), **c** magnetized water (30 min), **d** magnetized water (45 min), **e** magnetized water (60 min)

(Table 1). The result confirmed the purity of the obtained samples (Fig. 5 and inserted). (Yahya, there was no carbon in the precursor!). However, as the temperature was not uniform, no impurity was detected in the composition.

The typical N₂ adsorption–desorption isotherms (BET method) and the pore distribution curve of samples are depicted in Fig. 6. The samples were degassed before BET measurement based on the IUPAC recommendation for 16 h.

The micropores volume was calculated in the P/P₀ range of 0–0.990 to collect information about the type of porosity. BET surface activity and total pore volume (BJH method) were also considered. The hysteresis loop illustrates type-V indicating the formation of monolayer followed by multilayer and illustrates the presence of micropores. Moreover, the nanoparticle size was referenced to the mesoporous material; so the presence of mesoporous was proved [55]. The specific surface of the mesopores for both

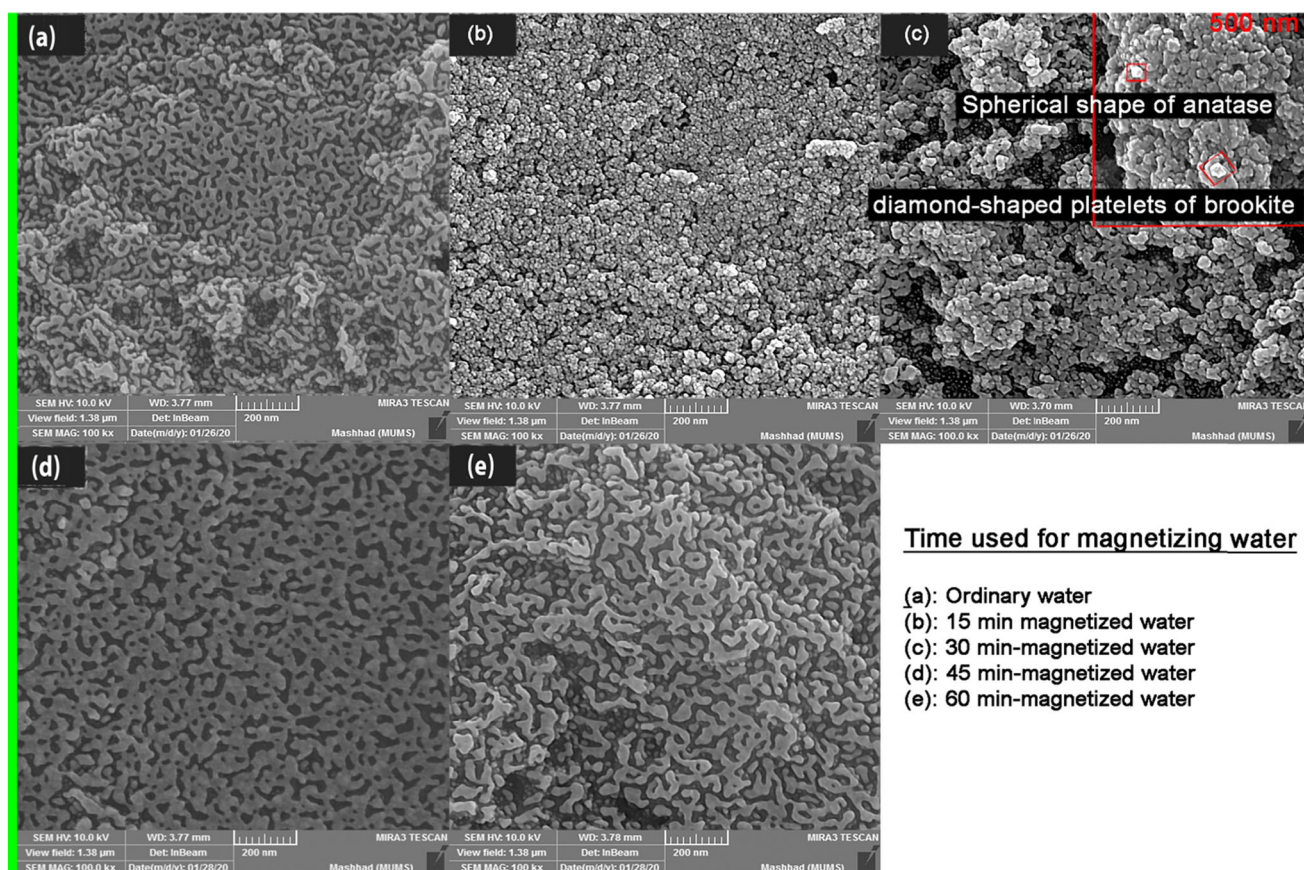


Fig. 4 FESEM image of the samples

Table 1 Elemental analysis by EDX method

Sample	O (weight %)	Ti (weight %)
TiO ₂ (used 30 min-magnetized water)	49.87	50.13

samples was calculated according to the differential molar adsorption work calculated from the adsorption–desorption isotherm (Table 2). The distribution of the adsorbent pore volume in terms of their diameters can be used to determine the maximum mesoporous diameter. All these data are listed in Table 2.

Adsorption phenomenon depends on both the adsorbate and adsorbent. Langmuir is one of the methods to describe the distribution of metal ion such as titanium between two phases of liquid and solid. According to this method, monolayer adsorption on the surface holds a limited number of adsorption sites with identical strategies with no transmigration of adsorbate in the plane surface. After filling the site, adsorption will not occur implying that the surface has no more volume and is

saturated. The data obtained from this analysis can be seen in Table 2.

The surface state of the TiO₂ nanoparticles was investigated by the FT-IR spectrum in the middle range of IR (400–4000 cm⁻¹) (Fig. 7). The absorptions between 3300 and 3400 cm⁻¹ are related to the stretching vibrations of adsorbed water molecules. Different types of H₂O molecule interacted with TiO₂ nanoparticles resulted the splitting the band into different components and assigning to formation of different types of H-bonds on the surface.

There is also another peak at ~ 1623 and 1626 cm⁻¹, which is related to (δ(OH)). The peaks at ~ 520 cm⁻¹ can be assigned to the Ti–O stretching in TiO₆ octahedras with several types of desorption.

TEM imaging was carried out for further morphological investigations (Fig. 8). As can be seen, the

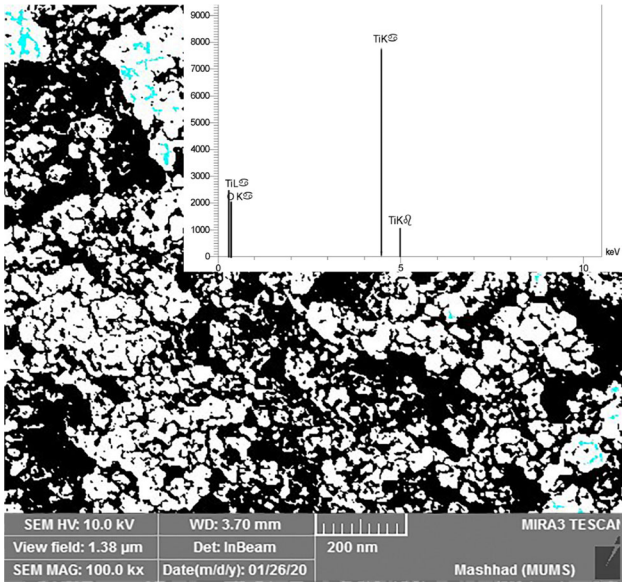


Fig. 5 EDX pattern of TiO₂ nanoparticle

brookite phase is the dominant phase (70–85%). TEM image also illustrates diamond-shaped platelets of brookite and few spherical anatase particles (15–30%). The brookite phase illustrates the basal faces matched to the [3 0 1] planes that are quasi-

perpendicular to planes [1 1 1] and [1 1 1]. There is also a plane of [0 2 0] as specified on the figure (Fig. 8, inserted). The mean size was obtained as 12 nm, which well matches the size obtained by XRD analysis.

4.2 Discussion

4.2.1 Effect of the magnetic field on the water

The pure water is a polar liquid. A part of the water has a negative electric charge, while the other is positively charged. As the water molecule is a tiny magnet (Bipolar), its magnetic field can be affected by forcing the molecule to rotate in another direction by placing it in a positive and negative potentials.

It has been proved that the positive electric charges make liquids softer [56] (not by reducing mineral compounds; but rather with less surface tension). The positive field makes all the obtained inorganic compounds hydrated through chopping liquid and solid compounds giving rise to crystals. Such imposed changes by the positive pole will influence the molecular structure and hence the crystallization of water molecules. Thus, it will increase hydration,

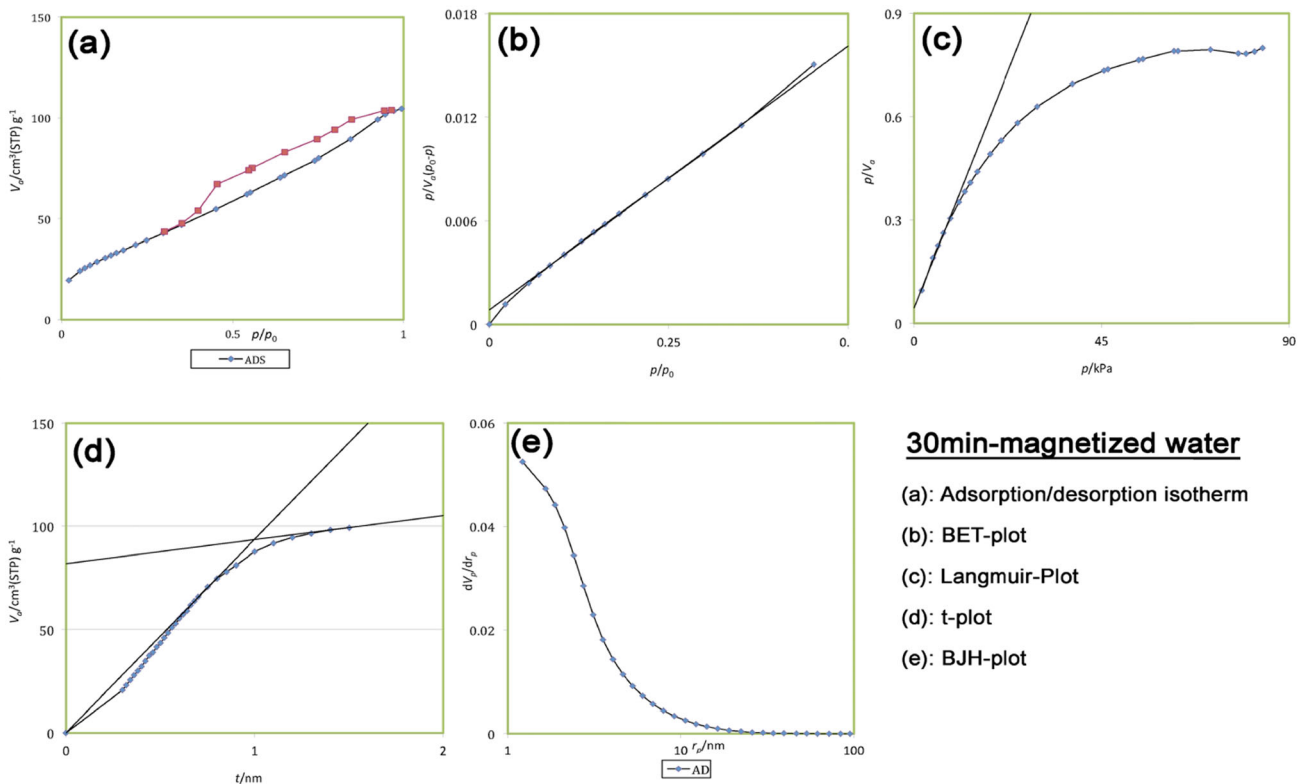


Fig. 6 Physical-chemical analysis of TiO₂ nanoparticles

30min-magnetized water

- (a): Adsorption/desorption isotherm
- (b): BET-plot
- (c): Langmuir-Plot
- (d): t-plot
- (e): BJH-plot

Table 2 Physical–chemical characterization of the samples (15 min and 30-min magnetized water)

Experiment's properties		
Sample weight [g]	0,0833	
Standard volume [cm ³]	9,779	
Dead volume [cm ³]	12,19	
Equilibrium time [sec]	0	
Adsorptive	N ₂	
Apparatus temperature [C]	0	
Adsorption temperature [K]	77.000	
BET		
15 min	30 min	
V_m [cm ³ (STP) g ⁻¹]	29,14	31,88
$a_{s,BET}$ [m ² g ⁻¹]	120,3	138,76
C	23,176	37,422
Total pore volume ($p/p_0 = 0.990$) [cm ³ g ⁻¹]	0,161	0,1616
Mean pore diameter [nm]	4,1624	4,6577
Langmuir plot		
15 min	30 min	
V_m [cm ³ (STP) g ⁻¹]	29,22	32,82
$a_{s,Lang}$ [m ² g ⁻¹]	137,6	142,85
B	0,5	0,6821
t- plot		
15 min	30 min	
a_1 [m ² g ⁻¹]	139,99	144,47
V_1 [cm ³ g ⁻¹]	0	0
a_2 [m ² g ⁻¹]	16,6	17,86
V_2 [cm ³ g ⁻¹]	0,1323	0,127
2θ [nm]	1,88	1,99
BJH plot		
15 min	30 min	
V_p [cm ³ g ⁻¹]	0,158	0,155
$r_{p,peak}(Area)$ [nm]	1,22	1,22
a_p [m ² g ⁻¹]	123,21	131,79

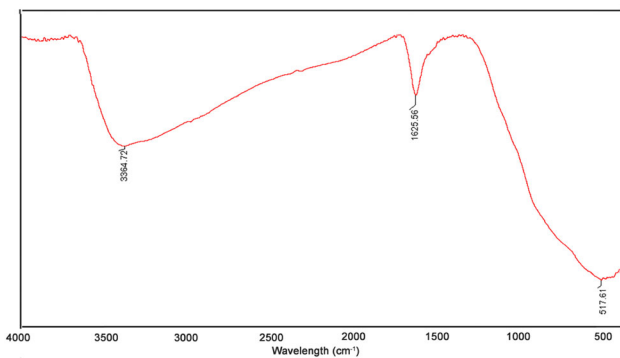


Fig. 7 FTIR spectroscopy of TiO₂ nanoparticle

solubility, and ionization ending up in physical, structural, and behavior changes in the liquid. Ion mobility will be also increased remarkably in water molecules. This phenomenon will enhance the flow of solvent liquid, accumulation of bigger particles;

the force obtained from the potential difference in processable solution is yield by 99.9% [57].

On the other hand, the negative pole (N pole) differently affects the liquids. After the liquid passed this pole, particles are accumulated, and hardness will increase the surface tension. This phenomenon can help in separation and precipitation. These changes in the electronic structure also influence the accumulation and crystallization of the water molecules and thus increase the hydration water, solubility, and ionization. These variations will physically, structurally, and behaviorally alter the liquid. Naturally, liquid molecules are located in an absolute accidental structure, due to the small natural changes in their pure electric charge. As polar substances, they react anomalously to electric influence depending on the pure charge of extra force. As an example, a positive charge influences the physical properties of

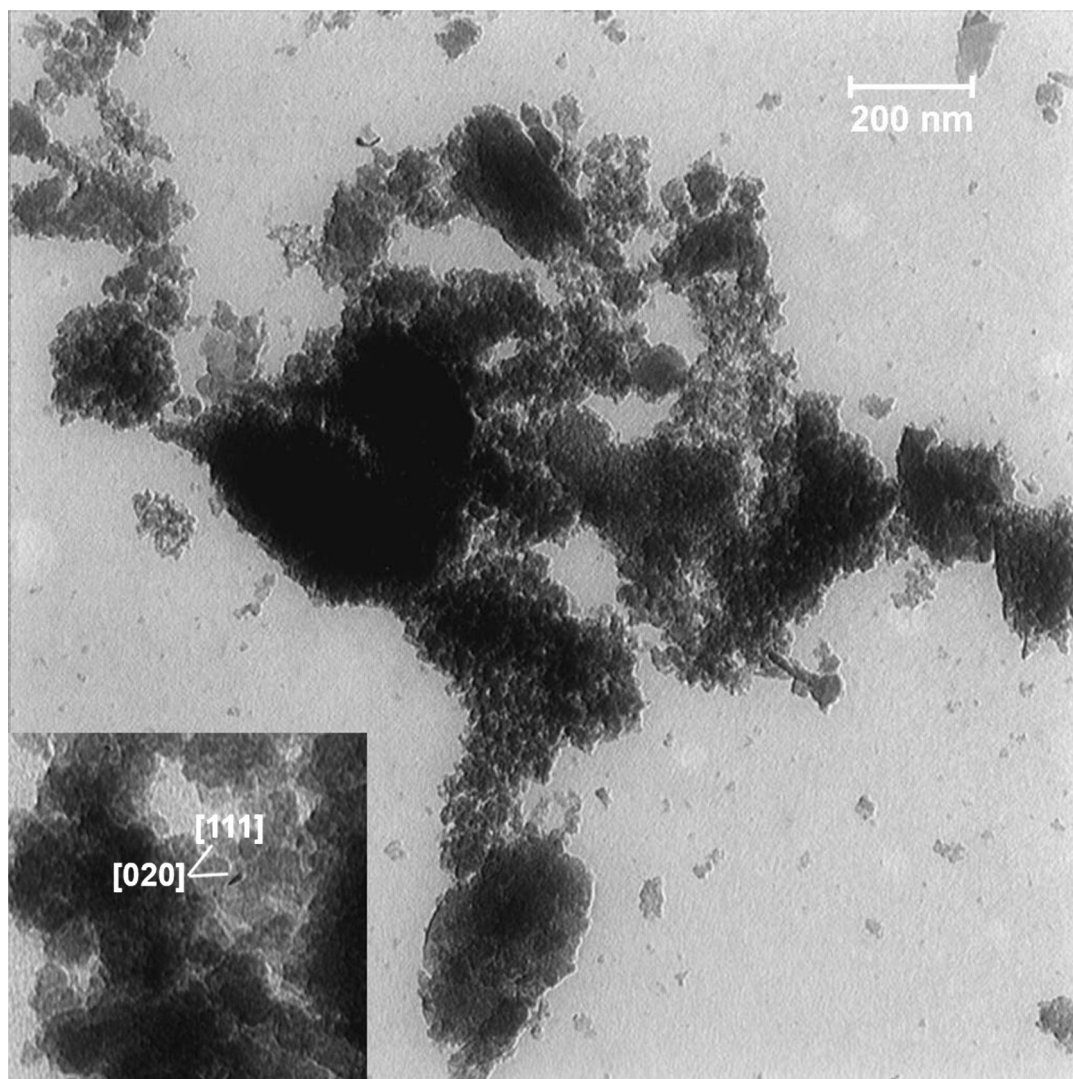


Fig. 8 The TEM image of TiO_2 nanoparticle

the liquid, so that the negative poles of molecules will be located in the nearest distance from the electric center (they absorb opposing charges and repel similar charges). After passing from the direct effect of extra electric force, molecules, with the highest pure-opposite charges, will be located in the nearest distance with the stimulus point, and inversely, the molecules with the highest identical pure charge will be situated in the farthest distance. The energized and amplified molecules, such as small magnets, become organized end to end, so that the energy of the pure charges becomes identical by the influence of extra magnet (Fig. 9). At the presence of a positive pole, electron rotation of atom is influenced giving rise to the electron orbital dense. In the case of water molecules, the hydrogen atoms are attracted to the

oxygen atoms by the electron sharing. It reduces the bond length, so the bonding angles change from the triangular structure to a linear one (Fig. 10). In this mode, hydrogen atoms become more positive and tend to support the negatively charged oxygen atoms. It changes the pure negative charge of the ordinary water molecule to the pure positive charge of magnetized water, so it alters the magnet of water pure charge [58]. Moreover, as the angle becomes smaller, more water molecules, and therefore oxygen can settle in a unit of volume, which is proper for the synthesis of TiO_2 with a more tense structure. Especially in the first step, when the aqueous complex of titanium is obtained (Eq. 2) with a stable state.

Another effect of the magnetic device is related to the acidic and alkaline phenomena. By the increase of

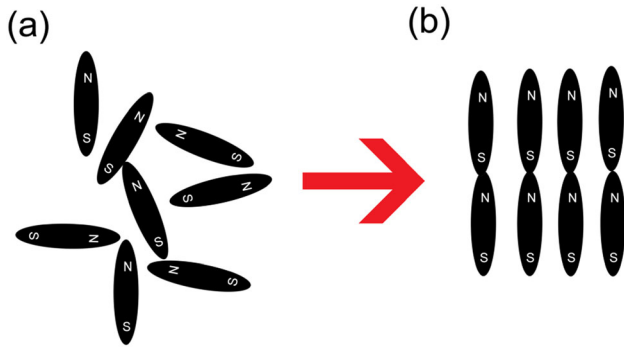


Fig. 9 The influence of magnetic field on the molecular structure; **a** before passing the magnetic field, **b** after passing the magnetic field water

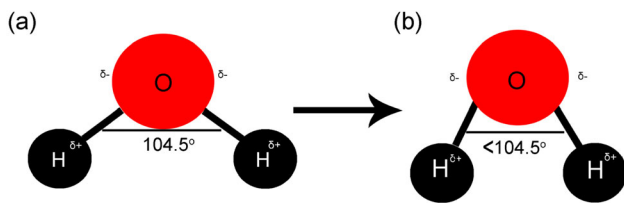


Fig. 10 The molecular structure of water; **a** before magnetizing, **b** after magnetizing

the magnetic device’s effect, the acidic liquid tends to the alkaline and alkaline liquid goes toward the acidic mode. This device reduces the surface tension of water without any reduction in its chemical properties. It provides better solubility of oxygen in the water and softens the water. In water treatment, treated water is specified by the surface tension. The analysis illustrates that the hard water has a surface tension of 71 din/cm^2 which declined to 62 din/cm^2 for the case of magnetized water.

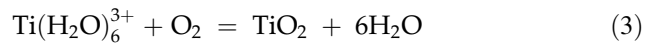
Water molecules are not designed individually, and they are attached by the hydrogen bonds. Whatever the molecules of water are less, their activity increases. The magnetic field decreases the number of mono-molecules, thus enhancing their activity [59].

4.2.1.1 Proposed mechanism for the formation of TiO_2 It is a novel and unique method, applied for the first time to synthesize TiO_2 nanoparticles. Indeed, synthesis of brookite TiO_2 at room temperature is a challenging task, as it is the second stable phase among all the phases of TiO_2 (Anatase > Brookite > Rutile) so it is hard to be formed without using high temperature Ti^{3+} is formed upon adding HCl to the solution of TiCl_3 ,

which then made an aqueous complex with the surrounding water (2) [60, 61]:



Adding NaOH turns the solution black from the light violet implying the formation of poly-cationic species due to a balance between Ti (III) and Ti (IV) [62, 63]. Further addition of NaOH ($\text{PH} \approx 9$) will result in some blue precipitates. These precipitates are almost oxidized substance, $\text{Ti}(\text{OH})_3^{+z}$, in which z is related to the oxidation rate. However, these solids were not stable and they became white after drying (50C, 24 h), as they turned into crystallized brookite.



4.2.1.2 The effect of the magnetized water in the formation of TiO_2 According to the previous work [44] and what we obtained in this project, upon using a magnetic field, the number of the hydrogen bond is increased due to the mentioned reason in the previous section; “the hydrogen atoms are attracted toward the oxygen atoms by the sharing electron. It reduces the bond length, so the bonding angles change from the triangular structure to the linear ones. In this mode, hydrogen atoms become more positive and tend to support the negatively charged oxygen atoms”. This is the main effective parameter, which makes a big difference between ordinary and magnetized water.

Another important phenomenon is the concentration of NaOH during the synthetic procedure. The use of high-concentration of NaOH weakens the net hydrogen bond; on the other hand, low-concentration of NaOH does not allow the precipitation. Here, the magnetic field can help. As it was mentioned that the usage of the magnetic field increases the number of the hydrogen bonds with no impact on the chemical reaction or stability of the bonds at high concentrations of NaOH.

Thus, based on the result, the magnetic field remarkably enhanced the stability and interaction force as compared to the ordinary water.

Moreover, the smaller the O–H bond, the bigger the cluster size. Therefore, the pack structure of the water molecule got closer [64]. It is worth noting that the usage of the magnetic field reduced the self-diffusion coefficient of the molecules, using a less step of solvent liquidity [44].

As the aim of this project was to use the magnetic field as an extra source to synthesis of TiO₂ nanoparticles, XRD and FESEM analysis were carried out under the same conditions. According to the result, the magnetic field interaction affected the growth of the nanoparticles, however, the use of the magnetic field for more than 30 min had a negative effect. It is also important to mention that the attraction force on the particles is much higher when the magnetic field is used, which can influence the product morphology.

For a deeper investigation of the behavior of the system at the magnetic field, RDF analysis was carried out on the oxygen of TiO₂ and the hydrogen atom of the water solvent. According to the analysis, there is a strong interaction between the oxygen atoms of TiO₂ and the hydrogen atom of water. It has been done for all the tests and the distances were 2.342 Å, 2.292 Å, 2.21 Å, 3.32 Å, and 3.41 Å for ordinary water and those magnetized for 15, 30, 45, and 60 min, respectively. The result showed the strongest interaction between the mentioned atoms in the case 30-min-magnetized water.

The mentioned results illustrate why magnetized water could influence the formation of TiO₂ nanoparticles. The reasons extracted from the “Effect of the magnetic field on the water” section provide information about the high formation of the precipitates. However, it should be mentioned that all the following reasons hold if they have a regular array in their molecular structure (See Fig. 9) and it has been obtained upon using the magnetic field.

- (I) “Positive field makes all the obtained inorganic compounds hydrated through chopping liquid and solid compounds resulting in crystal formation”
- (II) “After the liquid passed the negative pole field, particles are accumulated, and hardness will increase the surface tension. This phenomenon helps in separation and precipitation”. The precipitate is Ti(OH)_{3+z}, which then progresses to TiO₂.

5 Conclusion

TiO₂ was synthesized by a method, which is compatible with the environment through magnetized water, obtained from the US-patent device for the

first time. According to the result, 15- and 30-min magnetization resulted in the outcomes. However, 30 min magnetization could provide better conditions for obtaining TiO₂ at room temperature. Indeed, oxidation and precipitation resulted in the formation of TiO₂. Thus, by controlling the condition through water magnetization, it was possible to obtain TiO₂ with a desired crystal phase of brookite. Moreover, it was recognized it is possible to obtain ultra-small TiO₂ nanoparticle under a soft condition.

The proposed method is highly environmentally friendly and economic as it optimizes two important parameters in the industries: a short procedure that does not require high temperatures and using magnetized water as green solvent.

Acknowledgements

Funding for this research was provided by the Ministry of Education and Science of the Russian Federation (Award No. 075-03-2020-223 (FSSF-2020-0017)) and Ferdowsi University of Mashhad research Council.

Declaration

Conflict of interest The authors declare that they have no known competing financial interests or personal relationships that could have appeared to influence the work reported in this paper.

References

1. G. Zhou, Y. Cao, Y. Jin, C. Wang, Y. Wang, C. Hua, S. Wu, J. Clean. Prod. **274**, 122929 (2020)
2. N. Ahmadpour, M.H. Sayadi, S. Sobhani, M. Hajiani, J. Clean. Prod. **268**, 122023 (2020)
3. A.S. Abdulhameed, A.K.T. Mohammad, A.H. Jawad, J. Clean. Prod. **232**, 43 (2019)
4. M. A. de Bittencourt, A.M. Novack, J.A. Scherer Filho, L.P. Mazur, B.A. Marinho, A. da Silva, A.A.U. de Souza, S.M.A.G.U. de Souza, J. Clean. Prod. **268**, 122164 (2020)
5. I.C. Kang, Q. Zhang, S. Yin, T. Sato, F. Saito, Appl. Catal. B **80**, 81 (2008)
6. X. Wang, M. Sun, M. Murugananthan, Y. Zhang, L. Zhang, Appl. Catal. B **260**, 118205 (2020)
7. J. Xu, N. Liu, D. Wu, Z. Gao, Y.-Y. Song, P. Schmuki, ACS Nano **14**, 337 (2020)

8. W.-T. Kim, K.-H. Na, J.-K. Lee, I. Jang, D.-S. Choi, W.-Y. Choi, *J. Nanosci. Nanotechnol.* **19**, 1743 (2018)
9. C. Pei, J.-H. Zhu, F. Xing, *J. Clean. Prod.* **279**, 123590 (2020)
10. R. Nasi, S. Esposito, F. Freyria, M. Armandi, T. Gadhi, S. Hernandez, P. Rivolo, N. Ditaranto, B. Bonelli, *Materials (Basel)*. **12**, 937 (2019)
11. K.T. Lim, H.S. Hwang, *Am. Chem. Soc.* **20**, 2466 (2003)
12. B. Stieberova, M. Zilka, M. Ticha, F. Freiberg, P. Caramazana-González, J. McKechnie, E. Lester, *J. Clean. Prod.* **241**, 118325 (2019)
13. Y. Shi, B. Sun, X. Wang, and D. Guo, *Res. Appl. Mater. Sci.* **1**, (2019).
14. S.T. Rahmat, W.K. Tan, G. Kawamura, A. Matsuda, Z. Lockman, *J. Alloys Compd.* **812**, 152094 (2020)
15. B.N. Bhadra, J.Y. Song, N. Uddin, N.A. Khan, S. Kim, C.H. Choi, S.H. Jung, *Appl. Catal. B* **240**, 215 (2019)
16. M.T. Le, H.L. Nguyen, A. Vu, V.C. Nguyen, J.C.S. Wu, *J. Chin. Chem. Soc.* **66**, 1713 (2019)
17. Q. Zhang, C. Li, *Catal. Today* **9**(12), 990 (2019)
18. A.K. Singh, V. Chaudhary, A.K. Singh, S.R.P. Sinha, *Synth. Met.* **256**, 116155 (2019)
19. K. Kim, J. Park, H. Kim, G.Y. Jung, M.-G. Kim, *ACS Catal.* **9**, 9206 (2019)
20. (n.d.)
21. A. Vahl, S. Veziroglu, B. Henkel, T. Strunskus, O. Polonskyi, O.C. Aktas, F. Faupel, *Materials (Basel)*. **12**, 2840 (2019)
22. R. Sharma, A. Sarkar, R. Jha, A. Kumar Sharma, D. Sharma, *Int. J. Appl. Ceram. Technol. IJAC.* 13439 (2019)
23. S. Das, A. Ghosh, *J. Appl. Polym. Sci.* **5**, 48757 (2019)
24. I. Heng, C.W. Lai, J.C. Juan, A. Numan, J. Iqbal, E.Y.L. Teo, *Ceram. Int.* **45**, 4990 (2019)
25. A. Mehrizad, M.A. Behnajady, P. Gharbani, S. Sabbagh, *J. Clean. Prod.* **215**, 1341 (2019)
26. J. Tian, Q. Shao, J. Zhao, D. Pan, M. Dong, C. Jia, T. Ding, T. Wu, Z. Guo, *J. Colloid Interface Sci.* **541**, 18 (2019)
27. A.G.R. Howe, R. Maunder, D.J. Morgan, J.K. Edwards, *Catalysts* **9**, 748 (2019)
28. D.B. Dwyer, D.J. Cooke, M.F. Hidalgo, B. Li, J. Stanton, F. Omenya, W.E. Bernier, W.E. Jones, *J. Fluor. Chem.* **227**, 109375 (2019)
29. Y. Absalan, M.A. Ryabov, O.V. Kovalchukova, *Mater. Sci. Eng. C* **97**, 813 (2019)
30. Y. Absalan, E.A. Fortalnova, N.N. Lobanov, E.V. Dobrokhotova, O.V. Kovalchukova, *J. Organomet. Chem.* **859**, 80 (2018)
31. Y. Absalan, I.G. Bratchikova, O.V. Kovalchukova, *J. Mol. Liq.* **268**, 882 (2018)
32. Y. Absalan, I. Bratchikova, O.V. Kovalchukova, *Environ. Nanotechnol. Monit. Manag. J.* **8**, 244 (2017)
33. Y. Absalan, I. Bratchikova, Labanov, O.V.Kovalchukova, *J. Mater. Sci. Mater. Electron.* **28**, 18220 (2017)
34. Y. Absalan, O.V. Avramenko, O.V. Kovalchukova, *Butlerov Commun.* **47**, 49 (2016)
35. Z. Shayegan, C.-S. Lee, F. Haghghat, *Chem. Eng. J.* **334**, 2408 (2018)
36. A. Hashemizadeh, M.J. Amiri, B. Aminshahidi, M. Gholizadeh, *Corrosion 1* (2016).
37. Z. Eshaghi, M. Gholizadeh, *Talanta* **64**, 558 (2004)
38. G.H. Rounaghi, M. Gholizadeh, F. Moosavi, I. Razavipanah, H. Azizi-toupanloo, M.R. Salavati, *RSC Adv.* **6**, 9096 (2016)
39. M. Bakherad, F. Moosavi, R. Doosti, A. Keivanloo, M. Gholizadeh, *New J. Chem.* **42**, 4559 (2018)
40. M. Bakherad, R. Doosti, A. Keivanloo, M. Gholizadeh, *J. Iran. Chem. Soc.* **14**, 2591 (2017)
41. M. Bakherad, Z. Moosavi-Tekyeh, A. Keivanloo, M. Gholizadeh, Z. Toozandejani, *Res. Chem. Intermed.* **44**, 373 (2017)
42. M. Bakherad, R. Doosti, A. Keivanloo, M. Gholizadeh, A.H. Amin, *Lett. Org. Chem.* **14**, 510 (2017)
43. A.N. Pour, J. Karimi, M. Gholizadeh, *J. Iran. Chem. Soc.* **14**, 1477 (2017)
44. H. Rashidi, A. Ahmadpour, M. Gholizadeh, F.F. Bamoharram, F. Moosavi, *Adv. Powder Technol.* **29**, 349 (2018)
45. P.M.E. Parthiban, P.M.R.M.E, S. George, *Int. J. Eng. Res. Technol. ISSN* **4**, 65 (2016).
46. H. Afshin, M. Gholizadeh, N. Khorshidi, *Trans. A Civ. Eng.* **17**, 74 (2010)
47. S. Ghorbani, M. Gholizadeh, *Materials (Basel)*. **11**, 1 (2018)
48. M. Gholizadeh, H. Arabshahi, *J. Eng. Technol. Res.* **3**, 77 (2011)
49. A. Gilani, H. Kermanshahi, A. Golian, M. Gholizadeh, *Iran. J. Appl. Anim. Sci.* **3**, 687 (2013)
50. M. Gholizadeh, H. Arabshahi, M.R. Saeidi, B. Mahdavi, *Middle-East J. Cient. Res.* **3**, 140 (2008)
51. E. Esmaeilnezhad, H.J. Choi, M. Schaffie, M. Gholizadeh, M. Ranjbar, *J. Clean. Prod.* **171**, 45 (2018)
52. A. Gilani, H. Kermanshahi, M. Gholizadeh, *J. Arid. Agric.* **3**, 23 (2017)
53. M. Gholizadeh, US 10 507 450B2 (2019).
54. E. Esmaeilnezhad, H. Jin, M. Schaf, M. Gholizadeh, *J. Clean. Prod. J.* **161**, 908 (2017)
55. S. Mobini, F. Meshkani, M. Rezaei, *Process Saf. Environ. Prot.* **107**, 181 (2017)
56. B.S. Joshi, V.N. Kamat, *Tetrahedron Lett.* **7**, 5767 (1966)
57. M.R. Powell, *Skept. Inq.* **22**, (1998).
58. J. Zheng, P. Xu, M. Gu, J. Xiao, N.D. Browning, P. Yan, C. Wang, J.G. Zhang, *Chem. Mater.* **27**, 1381 (2015)
59. (n.d.)

60. E. Sum, M. Skyllas-Kazacos, *J. Power Sources* **15**, 179 (1985)
61. D.J. Cookson, T.D. Smith, J.R. Pilbrow, *Cancer Res.* **23**, 833 (1963)
62. K.W. Stephens, C. Orvig, *Inorg. Chim. Acta* **273**, 47 (1998)
63. Aa. N. F. Pecsok, B Y Robert L, *Inorg. Chem.* **1**, 155 (1968).
64. H. Hosoda, H. Mori, N. Sogoshi, A. Nagasawa, S. Nakabayashi, *J. Phys. Chem. A* **108**, 1461 (2004)

Publisher's Note Springer Nature remains neutral with regard to jurisdictional claims in published maps and institutional affiliations.